Abstract

The Central Valley of California (CVC) and Mid-Atlantic (MA) in the U.S. are critical sites for waterfowl species in the winter, providing feeding and roosting locations for many species. Mapping waterfowl distributions using weather radar aids in the targeted adaptive management of important waterfowl habitats. Highlighting these locations for wintering waterfowl is a critical first step to conservation success. Additionally, mapping waterfowl distributions on a broad scale improves food security by allowing government agencies and commercial poultry operations to better understand the interface between wild and domestic birds that is related to risk of highly pathogenic avian influenza outbreaks. Improving understanding of predictors of wintering waterfowl distributions at both local and landscape scales, will allow facility managers and regulatory agencies to make more informed risk management decisions. We used 9 years (2014–2023) of data from the US NEXRAD network to model winter waterfowl distributions in the CVC and MA as a function of weather, temporal, and environmental characteristics using boosted regression tree modelling. We were able to capture the variability in effect size of 28 different covariates across space and time within two geographic regions which are critical to nationwide waterfowl management and have a high density of commercial poultry. In general, environmental and geographic predictors had the strongest relative effect on predicting wintering waterfowl distributions in both regions, while effects of land cover composition were more regionally and temporally specific. Increased daily mean temperature was a major predictor of increasing waterfowl distributions in both regions throughout the winter. Increasing precipitation had differing effects within regions, increasing waterfowl densities in the MA, while decreasing in general within the CVC. Increasing waterfowl densities in the CVC are strongly tied to the flooding of the landscape and rice availability, whereas waterfowl in the MA, where water is less

limiting, are generally governed by waste grain availability and emergent wetland on the landscape. Waterfowl distributions in the MA were generally higher nearer to the Atlantic coast and lakes, while in the CVC they were higher nearer to lakes. Our findings promote understanding of the predictors of winter waterfowl densities in relationship with biosecurity of commercial poultry nationally.

Introduction

Both the Central Valley of California (hereafter CVC) and Mid-Atlantic (hereafter MA) host critical sites for waterfowl (order *Anseriformes* including ducks, geese, and swans) along their respective flyways during the winter. These sites provide refuge and nutrition, which support waterfowl through the winter. Anthropogenic impacts such as urban development, hydrological modifications, and wetland conversion to agriculture has led to an estimated loss of 90% of natural wetlands in the CVC (Buler et al. 2012, Fleskes et al. 2018). In the MA, approximately 78% have been lost within the Delmarva Peninsula (A 33,669km² landmass comprising Delaware, Maryland, and Virginia, surrounded by the Chesapeake and Delaware Bays) (Stubbs et al. 2020). Wetlands have declined in much of the contiguous United States (Dahl 1990, O'Neal et al. 2008, Randall et al. 2011), and although the Farm Bill has provided the impetus for many wetland restoration programs (i.e., Wetland Reserve Program), wetlands are still being lost and disturbed at concerning rates nationally (Nestlerode et al. 2009, Sieges et al. 2014, Sesser et al. 2018) and globally (Hoozemans et al. 1993, Gass et al. 2023). Human practices may modify waterfowl distributions and disrupt migration corridors (Xu et al. 2021).

From a food security perspective, avian influenza virus (AIV), which is a naturally circulating zoonotic disease in *Anseriformes* and *Charadriiformes*, poses a serious threat to livestock, human, and economic health (Bevins et al. 2014, Franklin et al. 2021). Globally, highly pathogenic (HP) AIV and response protocols by governments to stop the spread of HPAIV have resulted in the loss of many millions of poultry during outbreaks. In the U.S alone, the 2021–2024 outbreak of the H5N1 HPAIV led to the loss of ~81 million domestic birds at 456 commercial poultry facilities within 35 states (USDA-APHIS, 2024). The CVC and MA are critical to nationwide poultry production (Prosser et al. 2017, Delmarva Chicken Association 2022, North Carolina Poultry Federation 2022, California Poultry Federation 2022) and have not been immune to the outbreak. In commercial poultry, the CVC had 64 documented detections of HPAIV resulting in mortality or euthanization of more than 6.9M birds, while the MA had 109 detections impacting 2.9M birds (USDA, 2024).

Waterfowl contribute to AIV transmission over broad spatial scales (Humphreys et al. 2021, Bevins et al. 2022, Gass et al. 2023). Inland waters and other waterfowl habitats near poultry facilities are significant risk factors concerning waterfowl-domestic bird virus spread (Ahmad et al. 2022, Green et al. 2023). Waterfowl movement may transfer AIV from one location to another, while also increasing the likelihood of exchange from infected to uninfected individuals (Fouchier and Munster 2009, Wikramaratna et al. 2014). Wild waterfowl and shorebirds in fields adjacent to poultry facilities were indicated to increase the introduction risk of HPAIV subtype H5N1 by 7.6 times on average (Green et al. 2023, Patyk et al. 2023).

Distributional patterns of wintering waterfowl can be quantified remotely using weather surveillance radar (e.g., NEXRAD) that can differentiate birds from other reflectors in the airspace (Larkin 1991, Gauthreaux and Belser 1998, Diehl and Larkin 2005, Buler and Diehl

2009, Chilson et al. 2017, Gauthreaux and Diehl 2020). Wintering waterfowl typically engage in daily flights between roosting and feeding sites to secure the daily caloric requirements needed during the winter (Johnson et al. 2014, Gates et al. 2020). Instantaneous radar samples at the onset of these evening waterfowl feeding flights are strongly correlated with waterfowl distributions at the ground (Buler et al. 2012). Nearly all birds aloft detected by radar at this time are waterfowl (O'Neal et al. 2010), particularly dabbling ducks (Randall et al. 2011).

Our objective was to model the associations of weather, temporal, and environmental variables in explaining wintering waterfowl distributions in the MA and CVC using nine years (2014–2023) of historical radar data. We used both static (distance to features and habitat proportions) and dynamic (climatic and vegetative) covariates to predict waterfowl distributions in both regions. Modelling waterfowl distributions using dynamic covariates such as weather conditions and habitat quality/availability (i.e., flooded vs. unflooded fields) captures the spatial and temporal variability within the system and subsequently allows for improved predictions when compared to using static covariates alone.

Although both critically important areas for wintering waterfowl, the CVC and the MA are fundamentally different ecological systems. Modelling both regions not only allowed us to address these fundamental differences pertaining to wintering waterfowl ecology, but also to gain a better insight into the region-specific drivers of AI risk to the commercial poultry industry. Waterfowl respond quickly to changes in environmental conditions, particularly in the CVC, where wintering waterfowl migration is closely tied to rice (*Oryza sativa*) production (Elphick 2000, Elphick 2008, Buler et al. 2012, Fleskes et al. 2018), and managed flooding of rice fields in the winter provide habitat and available food resources for waterfowl (Elphick and Oring 1998, Elphick 2000). For this reason, we hypothesized waterfowl distributions in the CVC will

be influenced by rice production, particularly in the fall with the onset of post-harvest flooding (Acosta et al. 2021; see Dybala et al. 2017 for timing of rice flooding) and then in response to variable drawdown in late winter (Sesser et al. 2018). We hypothesized waterfowl distributions within the MA to be less governed by water availability and flooding, and more so by proximity to the coastline (Prosser et al. 2017), access to waste grain (*Zea spp.* and *Glycine spp.*, Hill and Frederick 1997, Jefferies et al. 2003, Johnson et al. 2014), and roosting locations (Sieges et al. 2014, Jankowiak et al. 2015). Additionally, our results and predictive maps will contribute to the the a near-real time web-based application that will allow for both a broad-scale regional view or fine-scale view (i.e., local farm address) to promote improved biosecurity practices (i.e., taking precautions to minimize transmission risks of infectious disease) to flocks, from potential AIV outbreaks attributed to waterfowl densities across the landscape (Acosta et al. 2021). This application is fully accessible to poultry facility managers, who can use information to help mitigate HPAIV transmission risk to their flocks.

Material and methods

Study Area

We analyzed archived data from 6 NEXRAD sites (Figure 1); three in each of the CVC and MA. The 3 CVC radars; KBBX [39.49553, -121.63162], and KDAX [38.50117, -121.67787] in the Sacramento Valley, and KHNX [36.31420, -119.63207] in the San Joaquin Valley, provide coverage for two-thirds of the CVC. This area is dominated by agricultural land (*Oryza sativa*), human development, and a mosaic of managed wetland complexes (Buler et al. 2012). The MA radar sites are KDOX [38.82572, -75.44027], located in Dover, Delaware, within a landscape of

high agricultural abundance (*Zea spp.*, *Glycine spp.,* and small grains) intermixed with poultry farms, wetland complexes, patchy woodland, estuarine bays, and wildlife management areas. KMHX [34.77588, -76.87625] in Newport, North Carolina and KLTX [33.98909, -78.42908] in Shallotte, North Carolina are dominated by ocean, bays, agriculture, rivers, estuarine inlets, large lakes, and forested wildlife management areas with dispersed, yet abundant human development.

Radar Analysis & Processing

We analyzed NEXRAD data between 1 November - 15 March 2014–2023 to estimate waterfowl densities spatially and temporally across the CVC and MA. Analysis of November – 15 March minimizes biological contamination of radar data caused by onset of land bird migration (Buler and Diehl 2009, Buler and Dawson 2014). The radars collect 5 to 14 horizontal 360° sweeps at vertical tilt angles ranging between 0.5° to 19.5°, into a volume scan (3D representation of the airspace). Volume scans are made every 5 to 10 min, depending on the radar's mode of operation ("precipitation" or "clean air" mode) (Ryzhkov and Zrnić 2019). Radar measures are gathered through the sending and receiving of horizontally polarized S-band (10 cm wavelength) radio waves at a peak power of 700KW (Diehl and Larkin 2005). NEXRAD radars have used horizontally and vertically polarized radio waves to obtain additional "dual polarization" measures since 2012 (Gauthreaux and Diehl 2020). Waterfowl biomass can be quantified via radar using reflectivity factor as the unit. The radar reflectivity factor measures the strength of a radar echo using dielectric properties of water in units of Z ($mm^6\, m^{-3}$) and is determined by the density and size of targets within the sampled volume.

Sampling Waterfowl Density

We used instantaneous samples of waterfowl density aloft from a subset of daily radar scans that coincided with the initiation of feeding flights at the end of evening civil twilight to quantify the ground sources from where waterfowl were departing. We used scans from the lowest elevation sweep (0.5°) and volume dimensions of 250 m long and 0.5° in diameter (Buler and Dawson 2014) to quantify waterfowl "on the ground" at the instant after initial ascent of feeding flights. Radar scans were selected contingent upon an initial manual pre-screening method. Specifically, we first visually screened radar scans for large-scale precipitation via NOAA's National Centers for Environmental Information Weather and Climate Toolkit (WCT). We then downloaded NEXRAD scans for precipitation-free nights via Amazon Web Services and further visually screened using the NOAA Weather and Climate Toolkit software. The screening process enabled us to remove days for analysis based on contaminating reflectivity from non-bird sources (i.e., precipitation, ground clutter, and anomalous propagation of the radar beam due to highly refractive atmospheric conditions (Buler et al. 2012). We visually screened 7,167 days of radar data from 6 radars, 46.41% (3,336) of which were classified as contamination free. We used data within individual sampling volumes of a radar domain where the radar beam sampled at least 10% of the vertical distribution of the birds in the airspace based on the vertical profile of reflectivity. Furthermore, the radar beam samples higher and broader heights with increasing range from the radar, creating a range bias in raw radar measures (Diehl and Larkin 2005). We corrected for range bias using the adjustment algorithm developed by Buler and Diehl (2009). For each sampling day, we sampled radar data at the sun angle at the instant of maximum rate of increase of mean reflectivity following McLaren et al. (2018). Reflectivity factor is measured in dBZ, which is converted into radar equivalent factor (Ze) [mm^6 m^{-3}]. Ze is then converted to total

bird reflectivity (η) [cm^2 km^{-3}] as a volumetric density (Chilson et al. 2017). Total bird

reflectivity is then quantified within 10 m interval altitudinal bins to produce a Vertical Profile of

Reflectivity (VPR; Buler and Diehl 2009, Buler et al. 2012). The VPR reflects the vertical

distribution of birds in the airspace and is constructed from reflectivity data from the five lowest

sweeps (tilt angle of 0.5° to 5.5°) and close (5–20 km) to the radar. The VPR is used to adjust

raw reflectivity measures for range bias to produce Vertically Integrated Reflectivity (VIR; Buler

and Diehl 2009; Buler and Dawson 2014). The VIR represents the mean cross-sectional area of

bird biomass across the entire column of air above the ground up to the height of the vertical

profile as in units of cm^2 ha^{-1}. We excluded areas of partial to total beam blockage and with

persistent clutter within each radar domain from further analyses (sensu Buler and Dawson

2014).

Model Analysis for Estimating Waterfowl Density

For each month of the season, we modelled the variability in mean daily VIR using Boosted

Regression Trees (BRTs) with 28 predictors. We aggregated daily VIR data into a 250 x 250 m

resolution grid and half-month time periods (i.e., bimonthly). Predictor variables consisted of 1)

ground elevation, 2) distance to features (e.g., radar, Atlantic coast, river, and lake), 3) land cover

proportion at local (250 m) and landscape (2 km) scales among ten land cover types, and 4)

weather variables (daily mean temperature, precipitation, vegetative greenness, soil wetness

index, and proportion of days with snow cover during each bimonthly period). We also included

a bimonthly period (early or late) for each month as a variable. We calculated distance to closest

features (coast, river, and lake) and used the USGS Digital Elevation model (U.S. Geological

Survey, 2023) to calculate relative ground elevation, which we defined as the elevation of the

radar minus the ground elevation in meters. Distance to the radar center was included as a

nuisance variable, given that the effect of increasing radar beam height and distance increases

waterfowl densities due to coverage of a larger volume. We used the United States Department of

Agriculture National Agricultural Statistics Service (USDA NASS) dataset at 30m x 30m

resolution to compute proportion of 10 land cover types (grain, rice [CVC specific], sod [MA

specific], emergent wetland, forested wetland, open water, grassland, forest, developed, and

shrub/scrub) at local and landscape scales. Types of agriculture were classified into either

grain/legume crops (corn, soybeans, rice, sweet corn, barley [*Hordeum vulgare]*, wheat [*Triticum*

aestivum], double crop winter wheat/soybean, alfalfa [*Medicago sativa]*, and other

hay/non-alfalfa) or sod (*Poaceae spp*).

We calculated mean daily temperature, using PRISM (Parameter-elevation Relationships

on Independent Slopes Model) Climate Group data (Oregon State University 2017). PRISM

datasets are modelled from over 10,000 surface stations across the United States using

climatologically aided interpolation with 4 km resolution. We calculated NDVI, using the

Vegetation Indexes-16-Days-250m resolution (M*D13Q1) MODIS (MODerate-resolution

Imaging Spectroradiometer) product. Soil wetness index was computed from the MODIS

reflectance data product MCD43A4 V005 (Nadir BRDF-Adjusted Reflectance), obtained from

the USGS LPDAAC (United States Geological Survey Land Processes Distributed Active

Archive Center). MCD43A4 V005 is produced every 16-days at 500-m resolution and contains

seven reflectance bands. We used the Tasseled cap transformation for MODIS data (Lobser and

Cohen 2007) to calculate a mean soil wetness index for each bimonthly period via the

tasseledCap function from the MODIS R package. Soil wetness index values > -0.05, and

approaching 0.125 are indicative of flooded habitat. Snow/Ice data was processed using the

Interactive Multisensor Snow and Ice Mapping System (IMS) Daily Northern Hemisphere Snow

and Ice Analysis at 1-km resolution. Region specific covariates for the MA included: distance to Atlantic coast, sod proportion (local and landscape scale), and snow/ice. For CVC, distance to the coast was not analyzed because it exceeds the NEXRAD detection range given that the study area is much further inland than the MA. Lastly, ground elevation was used in the CVC instead of the calculated relative ground elevation to reduce the effect of false reflectivity from the mountain ranges surrounding the valley.

We modelled densities of waterfowl across roosting areas using separate BRT models for each study area by month (November-March). We used a 250 x 250 m grid (same resolution as VIR data) and 28 covariates in modelling of each study area. To reduce the influence of spatial autocorrelation in modeling iterations, we partitioned grid cells into 25 groups in which sampled grid cells were 5 km apart and for each month combined covariate and radar data across years. We ran 25 BRT models (one for each grid partition subset) with the gbm.step function in R package '*dismo*' to model the relationship between log-mean VIR and environmental and landscape variables. Using fitted models, we computed predicted values of waterfowl densities for each grid cell and we created continuous surface layer maps of relative waterfowl roosting density throughout the study areas for each month (not shown here).

Results

Mean deviance explained of observed wintering waterfowl densities among models ranged from 39.3–68.7% in the MA (Table 1) and 54.5–72.2% in the CVC (Table 2). The top three biologically relevant (excluding distance from radar) predictors of waterfowl density were mean daily temperature, mean daily precipitation, and proportion of emergent wetland (landscape scale) in the MA and proportion of rice at the landscape scale, ground elevation, and mean daily

11

temperature in the CVC. The relative variable importance varied by month and region. In general, environmental factors were ranked highest, followed by geographic position, landscape-scale land cover, and local-scale land cover. Local scale land cover is not discussed in the results given its relatively low importance.

Environmental Variables

In the MA, there was a positive relationship between temperature and waterfowl density in all months. The strongest response between temperature and waterfowl density was in November and February (Figure 2A). Increasing precipitation increased waterfowl densities in November, February, and March (Figure 2B). Precipitation had the greatest relative importance during February. In the CVC, waterfowl densities increased as a function of increasing temperatures (Figure 2C), particularly in March and November. Opposite from the MA, waterfowl densities generally decreased in the CVC with increasing precipitation for all months except November (Figure 2D).

Landscape/Vegetative Conditions

Waterfowl densities in the MA were greater in drier (non-flooded) areas early and late in the season (November, December, and March), and greater within more flooded/open water habitat during mid-winter (January and February) (Figure 3A). In general, densities of waterfowl peaked within the MA for all months when NDVI values were below 0.4 (Figure 3B). For all months in the CVC, densities of waterfowl increased with relatively higher soil moisture index values and more area of flooded habitat across the landscape (Figure 3C); and for all months except November, the densities of waterfowl peaked with NDVI values between 0.5–0.7 (Figure 3D).

Geographic Location

In all months in the MA, with the exception of December, there was a bimodal relationship between distance from the coast and waterfowl densities. In December, waterfowl densities increased with greater proximity to the Atlantic coast (Figure 4A). For all other months of the winter, waterfowl densities were greatest at 0–10 km and again at 60–70 km from the coast. In the MA, waterfowl densities were relatively greater near lakes during November, December, and March, particularly at distances ≤ 2 km (Figure 4B). Similarly during January and February in the MA, higher densities of waterfowl were observed near lakes, but we also observed an increase in waterfowl densities at an average distance of 7.5-15 km from lakes. In the MA, with the exception of February, waterfowl densities were greatest at distances further away from rivers at a distance up to 35 km (Figure 4C). February also showed higher waterfowl counts in the MA at 35 km, but also had higher waterfowl densities at distances closer to rivers than any other month during the winter. In the CVC, the greatest concentrations of waterfowl occurred within the valley bottom and close to lakes (Figure 4D, E). In the CVC, the greatest waterfowl densities were observed when the distance from a lake was between 0–5 km (Figure 4E). In December, in the CVC, waterfowl densities increased at 20–25 km from lakes, in addition to higher densities at 0–5 km. In the CVC, there was a positive relationship between waterfowl densities and increasing distances from a river (Figure 4F). In November, in the CVC, highest waterfowl densities were observed at distances<2 km from rivers.

Landscape Scale Land Cover

For all land cover predictors and radar domains, wintering waterfowl exodus demonstrated the strongest response at the landscape (2 km) scale compared to the local scale (250 m). At the landscape scale within the MA, waterfowl densities were positively related to the proportion of emergent wetland in all months. The highest concentrations of waterfowl densities were in

November, December, and March when the proportion of emergent wetland was ~30–35% (Figure 5A). Waterfowl densities during January and February were greatest when emergent wetland proportion was ~60–65%. For all months, waterfowl densities were greatest when the proportion of shrub/scrub was low (0–5%) (Figure 5B). There was a weaker relationship between proportion of grassland and increasing waterfowl densities in November and December, but found that waterfowl densities increased in January, February, and March when proportions of grassland approached 20% (Figure 5C). Waterfowl densities increased for all months of the winter when proportion of grain increased (Figure 5D). The greatest waterfowl densities in all months of the winter were observed when the proportion of open water within 2 km was between 5–20% and then declined with greater open water extent (Figure 5E). There was a general increase in waterfowl density as proportion of developed land increased; however, there was a bimodal relationship where higher waterfowl densities were observed when proportion of development approached 0% (Figure 5F). For all winter months, waterfowl densities increased with decreasing proportions of forested land. The relationship between waterfowl densities and proportion of forest varied by month. In November, waterfowl densities increased as a function of increased proportion of forested wetlands between 0 and 10% forest and then declined with greater extent of forest. However, in December and January, waterfowl densities were greatest when proportion of emergent wetland were between 0–20% (Figure 5G).

In the CVC on the landscape scale, increasing waterfowl densities for all months with increasing proportions of rice (Figure 6A). The strength in response to rice was greatest during November and December and weakened as the winter progressed. The strength of response to rice by waterfowl in the CVC was consistently 3– 4 times greater than any other land cover type. Waterfowl densities increased in the CVC with increasing proportions of grassland, particularly

at around 75% within 2 km (Figure 6B). The greatest waterfowl densities within the CVC typically plateaued across all months when the proportion of developed land on the landscape reached 25–40% (Figure 6C). Similar to rice, but at a smaller scale, waterfowl densities increased with an increase in all other grain types on the landscape (Figure 6D). There was an increase in waterfowl densities in November and December with increasing proportions of emergent wetland on the landscape; however, between January-March, waterfowl densities varied very little with proportions of wetland between 25–80% (Figure 6E). Waterfowl densities consistently decreased within months in the CVC as a function of increasing open water on the landscape scale and the greatest waterfowl densities generally occurred when proportions of open water were ~20%, particularly in December and January (Figure 6F).

Discussion

Our analysis of diurnal wintering waterfowl distributions using weather radar observations reveal temporal and spatial variability in the directions and/or responses to important predictor variables within the Pacific and Atlantic Flyways. A consistent and major predictor of waterfowl distributions in both regions was mean daily temperature, which had a positive relationship with waterfowl densities at exodus. During months with migratory activity (e.g., November, February, March), this relationship is likely explained by temporal changes in the number of passage birds moving through the region. For example, autumn migration wanes as the month of November progresses. Thus, fewer passage migrants are detected later in the month when it is generally colder. This relationship is also likely explained by lower participation of birds in feeding flights on colder days within months. Mallards (*Anas platyrhynchos)*, like many wintering dabbling duck species, cease flight during extreme cold and resume high levels of activity again as a function of rising air temperature when the energy needed for thermoregulation is lower and fat

15

reserves need to be replenished (Jorde et al. 1983, 1984). There is variation by species and study site in response to temperature by wintering waterfowl regarding nocturnal exodus flights. Along the Seine estuary in France, Mallard and Eurasian Teal (*Anas crecca crecca*) fly further and consequently spend more time in the airspace with increasing temperatures (Legagneux et al. 2009). Additionally, Northern Pintail (*Anas acuta*) respond to winter progression rather than temperature in regard to duration and distance in flight, flying further as a function of winter progression and less far in warmer temperatures. In the Central flyway, interactive effects of seasonal progression and minimum temperature appear to be predictors of evening flight duration in Northern Pintail, Green-winged Teal (*Anas crecca*), American Wigeon (*Mareca americana*), and Mallard (Baldassarre and Bolen 1984), such that flight duration increased as a function of seasonal progression and colder temperatures. Opposite effects of temperature and flight during the evening are generally observed outside of the winter (i.e., during spring and fall migration) when cooler air in the airspace promotes more favorable flight conditions and opportunity for celestial navigation (Miller at al. 2005).

From an AIV epidemiological standpoint, cold freshwater (≤ 0°C) extends persistence of the virus in the environment (Ramey et al. 2022). Additionally, cold weather causes dabbling ducks to cease flight during exodus, often resulting in birds adopting more gregarious behaviors and increasing the chance of viral exchange (Longcore and Gibbs 1988). American Black Ducks (*Anas rubripes*) cease flight completely below 0°C and show a tendency to congregate together at temperatures below the species' lower critical temperature range (Longcore and Gibbs 1988). Dabbling ducks must take advantage of favorable weather conditions during the winter, particularly after a series of consecutive cold days, to replenish energy (lipid) supplies. In addition to the partial or complete cessation of flight and increase of gregarious behaviors, cold

16

weather during the winter also promotes AIV persistence in the environment (Brown et al. 2009). In general, North American dabbling ducks spend more time in flight compared to their European counterparts, with density dependent factors limiting food resources and increasing time spent scouting for new resources (Legagneux et al. 2009). Canada Geese (*Branta canadensis*) increase flight with temperatures $\geq$ -9°C (Raveling et al. 1972). Time spent in the airspace by Greater Snow Geese (*Chen caerulescens atlanticus*) was unrelated to temperature and precipitation in a previous study in the Delmarva Peninsula, although Greater Snow Geese fly slightly further on average in colder conditions (Hill and Frederick 1997).

Increasing wintering waterfowl density in the airspace with temperature could also be attributed to habitat availability, particularly in the MA, where frozen waterbodies may prohibit access to resources (Longcore and Gibbs 1988). In the CVC, extreme-cold induced cessation of flight by wintering waterfowl, even for smaller species, is far less likely and waterbodies are unlikely to freeze. Therefore, increased waterfowl densities observed at higher temperatures within the CVC may be explained by other additional factors. Artificial flooding of rice fields by farmers in California during the winter benefits a variety of waterbird species (Elphick and Oring 1998) by creating surrogate habitat in a landscape of water scarcity. Many dabbling duck species overwintering in the CVC have a preferred foraging depth range of 9–23 cm (Fredrickson 1991), and fluctuations in water depth caused by increased temperatures may shift the species composition that can access a certain site. Dabbling ducks may have to fly more to scout new sites if the current sites conditions are unfavorable. Increasing relative waterfowl densities and distributions as a function of increasing temperatures, particularly during late winter (February-March) in the CVC may be attributable to the access to new sources of nutrition. Increasing temperatures stimulate the growth of new grasses and shoots, and also increase

invertebrate abundance (Overton and Casazza 2023) which are important to geese and ducks respectively.

Precipitation was another major predictor of wintering waterfowl distributions, however with different effects by region. In the MA, precipitation was consistently positively associated with waterfowl densities throughout winter. In the CVC, for all months except at the start of winter (i.e., November), precipitation was negatively associated with waterfowl densities. Increasing waterfowl in response to increased precipitation in November could be closely tied to the artificial flooding of rice that often begins in November (Elphick 2000, Fleskes et al. 2018). We also found differing effects in the response to flooded habitats by waterfowl across the two regions, which we attribute to the comparatively differing open water availability in both regions. Precipitation and artificial flooding create functionally equivalent waterfowl habitats by providing refuge and a potential food source in agricultural waste grains (Elphick 2000). In the MA, we found a greater use of drier (non-flooded) sites earlier in the season (November-December), and then saw a progressive shift to use of flooded/open water habitat in January-March. Waterfowl density in the MA also increased during January-March as a function of increasing precipitation likely tied closely to the relationship with the soil wetness index and new influx of food provided by the flooding of the landscape (Elphick 2000). Sieges et al. (2014) found an opposite response in the Mississippi Alluvial Valley and West Gulf Coastal Plain, in which birds tend to favor flooded habitat throughout the entire winter, progressively moving to less flooded areas over time.

Soil wetness was a more important predictor in the CVC, likely given that water is a more limiting resource on the landscape and food availability in rice fields (a predominant habitat type in CVC) for ducks depends on fields being flooded. Waterfowl density increased

with greater soil wetness and peaks in flooded habitats as previously reported by Buler et al. (2012). The increased strength of response to flooded habitat in the CVC compared to the MA is likely due to habitat composition, water scarcity, and the practice of flooding rice after harvest (Elphick and Oring 1998, Fleskes et al. 2018), including the artificial flooding of habitat by the many duck clubs that exist within the region (Fleskes et al. 2018). In the MA, waterfowl densities decreased with increasing NDVI values for all months except January. In the MA, greatest waterfowl densities occurred at NDVI values between -0.1–0.25, which is indicative of water, barren land (i.e., crops), or sparse grassland (Elshehaby and Taha 2009). We found greatest densities of waterfowl within the CVC with NDVI values between 0.6–0.75 (i.e., grassland) in December-March, and between 0.3–0.4 (bare land) in November (Elshehaby and Taha 2009). We emphasize the need for region specific modelling, given the variation in species suite, habitat composition, and closely tied relationships with distinct agricultural systems (i.e., rice vs. corn/soybeans). Rice is the dominant form of agriculture in the CVC and its management practices greatly influence waterbird distributions (Elphick 2000). Rice is generally planted March-May and harvested in September-October. Post-harvest, machinery cuts and threshes the fields, and flooding is used as a waste decomposition mechanism (California Rice Commission 2023). Using water to decompose straw creates artificial wintering waterfowl habitat, providing nutrition and roosting locations critical to wintering waterfowl. In comparison, corn and soybeans are the dominant form of agriculture in the MA. Both crops are usually planted in May and harvested during September-October. The harvesting process leaves behind waste grain, which provides vital nutrition supplementation to waterfowl during the winter. Prior to the planting season, the spreading of waste on fields is occurring, which attracts other reservoir species such as gulls. Much of the corn and soybean production is used for domestic livestock

feed in the MA, which are often adjacent to the fields in which the crop is being grown, posing the opportunity for waterfowl and domestic animal interface.

In the MA, waterfowl were concentrated within 15 km of the coast, which supports the fact that the Delaware Bay, Chesapeake Bay, and the sounds (Albemarle and Pamlico) and bays (Onslow and Long) of North and South Carolinas support relatively high waterfowl densities during the winter (Madsen et al. 2013, Reese and Weterings 2018, Prosser et al. 2022). During the latter half of winter, we observed higher densities of waterfowl far (>60 km) from the coast, similar to the immediate coast. Inland detections of higher waterfowl densities in the MA are likely due to waterfowl using inland agricultural sites to feed and roost at inland lakes and impoundments, rather than coastal refuges. We found greater relative waterfowl densities closer to lakes in both the MA and CVC, which supports the hypothesis that inland water bodies support large numbers of roosting (Jankowiak et al. 2015) and feeding waterfowl. In addition to roosting locations, lakes also provide protection from mammalian predators (Fox and Kahlert 2000, Jankowiak et al. 2015).

Large lakes or impoundments close to agriculture provide crucial roosting sites and areas to rest and recover before flying out to feed. Important roosting sites closer to poultry facilities increase the risk of potential HPAIV outbreak (Iglesias et al. 2010). Smaller waterbodies, particularly in places where water availability is scarce (i.e., CVC), may lead to lower viral dilution and may promote increased opportunity for AIV transmission between individuals (Rohani et al. 2009, Pérez-Ramírez et al. 2012). In the MA, we saw many cases of GPS-fitted waterfowl directly and indirectly interfacing with poultry facilities and adjacent farm ponds, like situations previously observed for the CVC (McDuie et al. 2022).

In the CVC, we observed greater waterfowl densities with increasing distance from rivers approaching 60 km, with the exception of November, in which we observed higher waterfowl densities at sites both close to, and far from, rivers. The relationship between waterfowl densities and distance to rivers varied by month in the MA and CVC and could potentially be explained by the different suite of species present at different times during the winter using different resources. It is important to note that for both regions, predictions of waterfowl distributions in November and March may contain contamination from nocturnally migrating land birds, which are known to cluster along major geographical features such as rivers (Guo et al. 2023). Increased waterfowl observed near rivers in the MA during January and February could also be attributed to use of rivers by waterfowl when lakes are frozen. Inland waters near poultry farms are significant risk factors regarding HPAIV outbreaks at facilities (Ahmad et al. 2022). Rivers, streams, and regularly flooded land can support and facilitate the movement of H5N1 in and around nearby poultry facilities (Ward et al. 2009).

Regarding land cover factors that may increase waterfowl exposure to poultry facilities within the MA and CVC, the proportion of grain agriculture at the landscape scale was consistently positively related to waterfowl density. Waterfowl often require and take advantage of the surplus of agricultural waste grain at wintering sites (Hughes et al. 1994, Massé et al. 2001, Jefferies et al. 2003, Lefebvre et al. 2017, Gates et al. 2020) which often draws birds closer to adjacent poultry facilities (Elmberg et al. 2017). The risk of waterfowl-poultry interface within the MA and CVC will only increase as wetland is lost to agriculture and human development (Stubbs et al. 2020). Habitats in the MA with ~50% of wetland and proportion of open water not exceeding 20% at the landscape scale supported the highest densities of waterfowl. Grassland

proportions <10% and scrub/scrub habitat <5% at the landscape scale also appeared important to predicting waterfowl density.

In the CVC, increasing proportions of rice at the landscape scale was the most important predictor of waterfowl densities in early winter when overall waterfowl densities were at 8–9 times that of the rest of winter. The response strength of waterfowl to rice was 2–3 times greater during November and December, indicating the early season importance of rice to waterfowl in the CVC. On a much smaller scale, we found greater waterfowl densities when the proportion of grassland on the landscape in the CVC was ~70–75%, which is much higher than values in the MA. Graminoids, in addition to waste grains, are known to be a food source for wintering waterfowl, particularly for geese (Gauthier et al. 2005, Fan et al. 2020, Mott 2022). The response of increasing waterfowl densities to increasing proportions of emergent wetland (wetlands generally characterized by *Typha, Schoenoplectus, Pontederia, Peltandra, Polygonum* and *Carex spp*) at the landscape scale within the CVC was stronger during the earlier months (November-December). In the MA, the strongest response to emergent wetlands was during January and February. Many waterfowl and other waterbird species use emergent wetlands for roosting and feeding sites, and studies have shown waterbird densities to increase with more emergent wetlands on the landscape (Sieges et al. 2014). Agriculture and human development in both the MA and CVC have led to losses in natural wetlands (Fleskes et al. 2018, Stubbs et al. 2020, DeLuca et al. 2021), leading to declines in waterfowl populations (Fleskes et al. 2018), and an increase in interactions at the human-waterfowl interface (Cappelle et al. 2011, Elmberg et al. 2017, McDuie et al. 2022).

We observed a more dynamic response to the landscape within the CVC as compared with the MA. Waterfowl densities in the CVC were much greater and more concentrated

compared to the MA, with rice production and water resource availability a key driver of that particular ecosystem. Coastal sites, inland marshes, and the many natural and artificial waterbodies within the MA make water a far less limiting resource in the winter for waterfowl in the MA. In addition to habitat loss, water shortages force birds into larger congregations of multiple species at sites, which is known to facilitate AI transmission and emergence of highly pathogenic strains (Rohani et al. 2009, Wikramaratna et al. 2014), given that increasing water body size was found to be negatively associated with AI persistence in the environment (Ruiz et al. 2021). Research pertaining to depth as a function of AI prevalence may be biased and limited by samples taken in close proximity the shore (≤50 cm depth) given accessibility (Ahrens et al. 2023); however, deeper water may dilute the virus (Pérez-Ramírez et al. 2012, Numberger et al. 2019, Ahrens et al. 2023) and decelerate fecal-oral viral transmission in contrast to waterfowl aggregations in more shallow bodies of water (Pérez-Ramírez et al. 2012). High densities of birds in late November within the MA may be a combination of other known reservoirs of AIV, such as *Laridae* (Toennessen et al. 2011, Postnikova et al. 2021, Prosser et al. 2022)*, Scolopacidae* (Hall et al. 2014, Gass et al. 2023), *Sternidae* (Becker 1966, Rijks et al. 2022)*, Ardeidae* (Soda et al. 2022)*, Pelecanidae* (Lo et al. 2022, Beyit et al. 2023), or perhaps even the last wave of neotropical land bird migration. Higher reflectivity in November within the CVC and the comparatively large confidence intervals within estimates of fall migration in land birds within the CVC in September-October (DeLuca et al. 2021) is likely caused by the influx of waterfowl and other waterbirds (*Scolopacidae, Laridae, Sternidae, Ardeidae, Pelecanidae, Threskiornithidae, Gruidae,* and *Podicipedidae*), all of which have varying degrees of AI facilitation within the environment and between hosts. Waterfowl densities within the CVC in

November are closely tied to the annual flooding of rice (Elphick and Oring 1998, Elphick 2000, Fleskes et al. 2018.).

The 'California Waterfowl Tracker' (CWT) was introduced (Acosta et al. 2021), incorporating deterministic bird density models and daily environmental (precipitation, temperature, and subsequent wetness indices) variables to predict waterfowl location and density and AIV risk throughout the wintering period. Although the CWT application showed promise for the biosecurity of the Californian poultry industry, the underlying waterfowl distribution model is not representative of other regions or as a broad-scale application and is thus geographically limited. Our research improved the spatial and temporal resolution over the models from Acosta et al. (2021). We were able to demonstrate the differences in drivers of waterfowl distributions in different regions, which has previously been a challenge when implementing biosecurity strategies on a national level. Being able to incorporate temporal variability into region specific models will allow future managers to make more informed decisions as it pertains to the environment in which they operate poultry production units. In the Delmarva Peninsula, which falls within the MA, there were seven H5N1 outbreaks at commercial poultry facilities between 22 February – 8 March 2022, leading to a combined loss of ~3.2 million poultry. Therefore, our findings suggest that careful consideration be taken regarding the timing of poultry production practices in areas with high densities of waterfowl. Predictive modeling of waterfowl distributions will further allow for strategic decision-making by the poultry industry regarding potential exposure to farms or pertaining to new farm placement.

References

Acosta, S., T. Kelman, S. Feirer, E. Matchett, J. Smolinsky, M. Pitesky, and J. Buler. 2021. Using
the California Waterfowl Tracker to Assess Proximity of Waterfowl to Commercial
Poultry in the Central Valley of California. Avian Diseases 65:483–492.

Ahmad, S., K. Koh, D. Yoo, G. Suh, J. Lee, and C.-M. Lee. 2022. Impact of inland waters on
highly pathogenic avian influenza outbreaks in neighboring poultry farms in South
Korea. Journal of Veterinary Science 23:e36.

Ahrens, A. K., H.-C. Selinka, C. Wylezich, H. Wonnemann, O. Sindt, H. H. Hellmer, F. Pfaff, D.
Höper, T. C. Mettenleiter, M. Beer, and T. C. Harder. 2023. Investigating Environmental
Matrices for Use in Avian Influenza Virus Surveillance—Surface Water, Sediments, and
Avian Fecal Samples. D. R. Perez, editor. Microbiology Spectrum e02664-22.

Baldassarre, G. A., and E. G. Bolen. 1984. Field-Feeding Ecology of Waterfowl Wintering on the
Southern High Plains of Texas. The Journal of Wildlife Management 48:63–71.

Becker, W. B. 1966. The isolation and classification of Tern virus: influenza A-Tern South
Africa--1961. The Journal of Hygiene 64:309–320.

Bevins, S. N., K. Pedersen, M. W. Lutman, J. A. Baroch, B. S. Schmit, D. Kohler, T. Gidlewski,
D. L. Nolte, S. R. Swafford, and T. J. DeLiberto. 2014. Large-Scale Avian Influenza
Surveillance in Wild Birds throughout the United States. K.-J. Yoon, editor. PLoS ONE
9:e104360.

Bevins, S. N., S. A. Shriner, J. C. Cumbee, K. E. Dilione, K. E. Douglass, J. W. Ellis, M. L.
Killian, M. K. Torchetti, and J. B. Lenoch. 2022. Intercontinental Movement of Highly
Pathogenic Avian Influenza A(H5N1) Clade 2.3.4.4 Virus to the United States, 2021.
Emerging Infectious Diseases 28:1006–1011.

Beyit, A. D., I. K. Meki, Y. Barry, M. L. Haki, A. El Ghassem, S. M. Hamma, N. Abdelwahab, B. Doumbia, H. Ahmed Benane, D. S. Daf, Z. E. A. Sidatt, L. Ould Mekhalla, B. El Mamy, M. O. B. Gueya, T. B. K. Settypalli, H. Ouled Ahmed Ben Ali, S. Datta, G. Cattoli, C. E. Lamien, and W. G. Dundon. 2023. Avian influenza H5N1 in a great white pelican (Pelecanus onocrotalus), Mauritania 2022. Veterinary Research Communications. <https://doi.org/10.1007/s11259-023-10100-6>. Accessed 17 Apr 2023.

Brown, J. D., G. Goekjian, R. Poulson, S. Valeika, and D. E. Stallknecht. 2009. Avian influenza virus in water: Infectivity is dependent on pH, salinity and temperature. Veterinary Microbiology 136:20–26.

Buler, J. J., W. Barrow, and L. A. Randall. 2012. Wintering waterfowl respond to Wetlands Reserve Program lands in the Central Valley of California. CEAP Conservation Insight. CEAP Conservation Insight (NRCS). <https://pubs.er.usgs.gov/publication/70039733>. Accessed 13 Apr 2022.

Buler, J. J., and D. K. Dawson. 2014. Radar analysis of fall bird migration stopover sites in the northeastern U.S. The Condor.

Buler, J. J., and R. H. Diehl. 2009. Quantifying Bird Density During Migratory Stopover Using Weather Surveillance Radar. IEEE Transactions on Geoscience and Remote Sensing 47:2741–2751.

Cappelle, J., N. Gaidet, S. Iverson, J. Y. Takekawa, S. Newman, B. Fofana, and M. Gilbert. 2011. Characterizing the interface between wild ducks and poultry to evaluate the potential of transmission of avian pathogens. International Journal of Health Geographics. <https://agritrop.cirad.fr/563441/>. Accessed 16 Jan 2023.

Chilson, P. B., W. F. Frick, J. F. Kelly, and F. Liechti, editors. 2017. Aeroecology. Springer

    International Publishing, Cham. <http://link.springer.com/10.1007/978-3-319-68576-2>.

    Accessed 3 Jan 2023.

DeLuca, W. V., T. Meehan, N. Seavy, A. Jones, J. Pitt, J. L. Deppe, and C. B. Wilsey. 2021. The

    Colorado River Delta and California's Central Valley are critical regions for many

    migrating North American landbirds. Ornithological Applications 123:duaa064.

Diehl, R. H., and R. P. Larkin. 2005. Introduction to the WSR-88D (NEXRAD) for

    Ornithological Research. 13.

Elmberg, J., C. Berg, H. Lerner, J. Waldenström, and R. Hessel. 2017. Potential disease

    transmission from wild geese and swans to livestock, poultry and humans: a review of the

    scientific literature from a One Health perspective. Infection Ecology & Epidemiology

    7:1300450.

Elphick, C. S. 2000. Functional Equivalency between Rice Fields and Seminatural Wetland

    Habitats. Conservation Biology 14:181–191.

Elphick, C. S. 2008. Landscape Effects on Waterbird Densities in California Rice Fields:

    Taxonomic Differences, Scale-Dependence, and Conservation Implications. Waterbirds:

    The International Journal of Waterbird Biology 31:62–69.

Elphick, C. S., and L. W. Oring. 1998. Winter management of Californian rice fields for

    waterbirds. Journal of Applied Ecology 35:95–108.

Elshehaby, A., and L. Taha. 2009. A new expert system module for Building detection in urban

    areas using spectral information and LIDAR data. Applied Geomatics 1:97–110.

Fan, Y., L. Zhou, L. Cheng, Y. Song, and W. Xu. 2020. Foraging behavior of the Greater White-fronted Goose (Anser albifrons) wintering at Shengjin Lake: diet shifts and habitat use. Avian Research 11:3.

Fleskes, J. P., M. L. Casazza, C. T. Overton, E. L. Matchett, and J. L. Yee. 2018. Changes in the abundance and distribution of waterfowl wintering in the Central Valley of California, 1973–2000. Pages 50–74 *in*. Trends and Traditions: Avifaunal Change in Western North America. Western Field Ornithologists. <https://westernfieldornithologists.org/docs/2020/Avifaunal_Change/Fleskes/Fleskes-Avifaunal_Change.pdf>. Accessed 25 May 2023.

Fouchier, R. a. M., and V. J. Munster. 2009. Epidemiology of low pathogenic avian influenza viruses in wild birds. Revue Scientifique Et Technique (International Office of Epizootics) 28:49–58.

Fox, A. D., and J. Kahlert. 2000. Do moulting Greylag Geese Anser anser forage in proximity to water in response to food availability and/or quality? Bird Study 47:266–274.

Franklin, A. B., S. N. Bevins, and S. A. Shriner. 2021. Pathogens from Wild Birds at the Wildlife–Agriculture Interface. Pages 207–228 *in*. Infectious Disease Ecology of Wild Birds. Oxford University Press. <https://academic.oup.com/book/41220/chapter/350691909>. Accessed 3 Jan 2023.

Fredrickson, L. H. 1991. 13.4.6. Strategies for Water Level Manipulations in Moist-soil Systems.

Gass, J. D., R. J. Dusek, J. S. Hall, G. T. Hallgrimsson, H. P. Halldórsson, S. R. Vignisson, S. B. Ragnarsdottir, J. E. Jónsson, S. Krauss, S.-S. Wong, X.-F. Wan, S. Akter, S. Sreevatsan, N. S. Trovão, F. B. Nutter, J. A. Runstadler, and N. J. Hill. 2023. Global dissemination of

influenza A virus is driven by wild bird migration through arctic and subarctic zones. Molecular Ecology 32:198–213.

Gates, R. J., D. F. Caithamer, W. E. Moritz, and T. C. Tacha. 2020. Bioenergetics and Nutrition of Mississippi Valley Population Canada Geese during Winter and Migration. 68.

Gauthier, G., J.-F. Giroux, A. Reed, A. Bechet, and L. Belanger. 2005. Interactions between land use, habitat use, and population increase in greater snow geese: what are the consequences for natural wetlands? Global Change Biology 11:856–868.

Gauthreaux, S. A., and C. G. Belser. 1998. Displays of Bird Movements on the WSR-88D: Patterns and Quantification*. Weather and Forecasting 13:453–464.

Gauthreaux, S., and R. Diehl. 2020. Discrimination of Biological Scatterers in Polarimetric Weather Radar Data: Opportunities and Challenges. Remote Sensing 12:545.

Green, A. L., M. Branan, V. L. Fields, K. Patyk, S. K. Kolar, A. Beam, K. Marshall, R. McGuigan, M. Vuolo, A. Freifeld, M. K. Torchetti, K. Lantz, and A. H. Delgado. 2023. Investigation of risk factors for introduction of highly pathogenic avian influenza H5N1 virus onto table egg farms in the United States, 2022: a case–control study. Frontiers in Veterinary Science 10. <https://www.frontiersin.org/articles/10.3389/fvets.2023.1229008>. Accessed 27 Jul 2023.

Guo, F., J. J. Buler, J. A. Smolinsky, and D. S. Wilcove. 2023. Autumn stopover hotspots and multiscale habitat associations of migratory landbirds in the eastern United States. Proceedings of the National Academy of Sciences 120:e2203511120.

Hall, J. S., G. T. Hallgrimsson, K. Suwannanarn, S. Sreevatsen, H. S. Ip, E. Magnusdottir, J. L. TeSlaa, S. W. Nashold, and R. J. Dusek. 2014. Avian influenza virus ecology in Iceland

shorebirds: Intercontinental reassortment and movement. Infection, Genetics and Evolution 28:130–136.

Hill, M. R. J., and R. B. Frederick. 1997. Winter Movements and Habitat Use by Greater Snow Geese. The Journal of Wildlife Management 61:1213.

Hoozemans, F.M.J., M. Marchand, and H.A. Pennekamp. 1993. A global vulnerability analysis: Vulnerability Assessment for Population, Coastal Wetlands, and Rice Production on a Global Scale. 2nd Edition. Delft Hydraulics, the Netherlands.

Hughes, R. J., A. Reed, and G. Gauthier. 1994. Space and Habitat Use by Greater Snow Goose Broods on Bylot Island, Northwest Territories. The Journal of Wildlife Management 58:536.

Humphreys, J. M., D. C. Douglas, A. M. Ramey, J. M. Mullinax, C. Soos, P. Link, P. Walther, and D. J. Prosser. 2021. The spatial–temporal relationship of blue‑winged teal to domestic poultry: Movement state modelling of a highly mobile avian influenza host. Journal of Applied Ecology 58:2040–2052.

Iglesias, I., M. J. Muñoz, M. Martínez, and A. de la Torre. 2010. Environmental Risk Factors Associated with H5N1 HPAI in Ramsar Wetlands of Europe. Avian Diseases 54:814–820.

Jankowiak, Ł., P. Skórka, Ł. Ławicki, P. Wylegała, M. Polakowski, A. Wuczyński, and P. Tryjanowski. 2015. Patterns of occurrence and abundance of roosting geese: the role of spatial scale for site selection and consequences for conservation. Ecological Research 30:833–842.

Jefferies, R. L., R. F. Rockwell, and K. F. Abraham. 2003. The embarrassment of riches: agricultural food subsidies, high goose numbers, and loss of Arctic wetlands — a continuing saga. 11:41.

Johnson, W. P., P. M. Schmidt, and D. P. Taylor. 2014. Foraging flight distances of wintering

ducks and geese: a review. Avian Conservation and Ecology 9:art2.

Jorde, D. G., G. L. Krapu, and R. D. Crawford. 1983. Feeding Ecology of Mallards Wintering in

Nebraska. The Journal of Wildlife Management 47:1044–1053.

Jorde, D. G., G. L. Krapu, R. D. Crawford, and M. A. Hay. 1984. Effects of Weather on Habitat

Selection and Behavior of Mallards Wintering in Nebraska. The Condor 86:258–265.

Larkin, R. P. 1991. 25TH INTERNATIONAL CONFERENCE ON RADAR METEOROLOGY

JUNE 24–28, 1991, PARIS, FRANCE. Bulletin of the American Meteorological Society

72:285–319.

Lefebvre, J., G. Gauthier, J.-F. Giroux, A. Reed, E. T. Reed, and L. Bélanger. 2017. The greater

snow goose Anser caerulescens atlanticus: Managing an overabundant population. Ambio

46:262–274.

Legagneux, P., C. Blaize, F. Latraube, J. Gautier, and V. Bretagnolle. 2009. Variation in

home-range size and movements of wintering dabbling ducks. Journal of Ornithology

150:183–193.

Lo, F. T., B. Zecchin, A. A. Diallo, O. Racky, L. Tassoni, A. Diop, Moussa Diouf, Mayékor

Diouf, Y. N. Samb, A. Pastori, F. Gobbo, F. Ellero, M. Diop, M. M. Lo, M. N. Diouf, M.

Fall, A. A. Ndiaye, A. M. Gaye, M. Badiane, M. Lo, B. N. Youm, I. Ndao, M. Niaga, C.

Terregino, B. Diop, Y. Ndiaye, A. Angot, I. Seck, M. Niang, B. Soumare, A. Fusaro, and

I. Monne. 2022. Intercontinental Spread of Eurasian Highly Pathogenic Avian Influenza

A(H5N1) to Senegal. Emerging Infectious Diseases 28:234–237.

Lobser, S. E., and W. B. Cohen. 2007. MODIS tasselled cap: land cover characteristics expressed through transformed MODIS data. International Journal of Remote Sensing. 28(22): 5079-5101 28:5079–5101.

Longcore, J. R., and J. P. Gibbs. 1988. Distribution and Numbers of American Black Ducks along the Maine Coast during the Severe Winter of 1980–1981. Waterfowl in Winter 377–390.

Madsen, J. M., N. G. Zimmermann, J. Timmons, and N. L. Tablante. 2013. Avian Influenza Seroprevalence and Biosecurity Risk Factors in Maryland Backyard Poultry: A Cross-Sectional Study. F. C. C. Leung, editor. PLoS ONE 8:e56851.

Massé, H., L. Rochefort, and G. Gauthier. 2001. Carrying Capacity of Wetland Habitats Used by Breeding Greater Snow Geese. The Journal of Wildlife Management 65:271–281.

McDuie, F., E. L. Matchett, D. J. Prosser, J. Y. Takekawa, M. E. Pitesky, A. A. Lorenz, M. M. McCuen, O. C. T, J. T. Ackerman, S. E. W. De La Cruz, and M. L. Casazza. 2022. Pathways for avian influenza virus spread: GPS reveals wild waterfowl in commercial livestock facilities and connectivity with the natural wetland landscape. Transboundary and Emerging Diseases 69:2898–2912.

McLaren, J. D., J. J. Buler, T. Schreckengost, J. A. Smolinsky, M. Boone, E. Emiel van Loon, D. K. Dawson, and E. L. Walters. 2018. Artificial light at night confounds broad-scale habitat use by migrating birds. Ecology Letters 21:356–364.

Miller, M. R., J. Y. Takekawa, J. P. Fleskes, D. L. Orthmeyer, M. L. Casazza, D. A. Haukos, and W. M. Perry. 2005. Flight Speeds of Northern Pintails during Migration Determined Using Satellite Telemetry. The Wilson Bulletin 117:364–374.

Mott, A. L. 2023. Habitat Use and Distribution Implications of Four Goose Species Wintering in California's Sacramento Valley.

Nestlerode, J.A., V.D. Engle, P. Bourgeois, P.T. Heitmuller, J.M. Macauley, and Y.C. Allen. 2009. An integrated approach to assess broad-scale condition of coastal wetlands: The Gulf of Mexico coastal wetlands pilot survey. Environmental Monitoring and Assessment 150:21–29.

Numberger, D., C. Dreier, C. Vullioud, G. Gabriel, A. D. Greenwood, and H.-P. Grossart. 2019. Recovery of influenza A viruses from lake water and sediments by experimental inoculation. J. Waldenström, editor. PLOS ONE 14:e0216880.

O'neal, B. J., E. J. Heske, and J. D. Stafford. 2008. Waterbird Response to Wetlands Restored Through the Conservation Reserve Enhancement Program. The Journal of Wildlife Management 72:654–664.

O'Neal, B. J., J. D. Stafford, and R. P. Larkin. 2010. Waterfowl on weather radar: applying ground-truth to classify and quantify bird movements. Journal of Field Ornithology 81:71–82.

Overton, C. T., and M. L. Casazza. 2023. Movement behavior, habitat selection, and functional responses to habitat availability among four species of wintering waterfowl in California. Frontiers in Ecology and Evolution 11. <https://www.frontiersin.org/articles/10.3389/fevo.2023.1232704>. Accessed 30 Oct 2023.

Patyk, K. A., V. L. Fields, A. L. Beam, M. A. Branan, R. E. McGuigan, A. Green, M. K. Torchetti, K. Lantz, A. Freifeld, K. Marshall, and A. H. Delgado. 2023. Investigation of risk factors for introduction of highly pathogenic avian influenza H5N1 infection among

commercial turkey operations in the United States, 2022: a case-control study. Frontiers in Veterinary Science 10. <https://www.frontiersin.org/articles/10.3389/fvets.2023.1229071>. Accessed 30 Aug 2023.

Pérez-Ramírez, E., P. Acevedo, A. Allepuz, X. Gerrikagoitia, A. Alba, N. Busquets, S. Díaz-Sánchez, V. Álvarez, F. X. Abad, M. Barral, N. Majó, and U. Höfle. 2012. Ecological Factors Driving Avian Influenza Virus Dynamics in Spanish Wetland Ecosystems. PLOS ONE 7:e46418.

Postnikova, Y., A. Treshchalina, E. Boravleva, A. Gambaryan, A. Ishmukhametov, M. Matrosovich, R. A. M. Fouchier, G. Sadykova, A. Prilipov, and N. Lomakina. 2021. Diversity and Reassortment Rate of Influenza A Viruses in Wild Ducks and Gulls. Viruses 13:1010.

Prosser, D. J., J. Chen, C. A. Ahlstrom, A. B. Reeves, R. L. Poulson, J. D. Sullivan, D. McAuley, C. R. Callahan, P. C. McGowan, J. Bahl, D. E. Stallknecht, and A. M. Ramey. 2022. Maintenance and dissemination of avian-origin influenza A virus within the northern Atlantic Flyway of North America. R. A. M. Fouchier, editor. PLOS Pathogens 18:e1010605.

Prosser, D. J., C. L. Densmore, L. J. Hindman, D. D. Iwanowicz, C. A. Ottinger, L. R. Iwanowicz, C. P. Driscoll, and J. L. Nagel. 2017. Low Pathogenic Avian Influenza Viruses in Wild Migratory Waterfowl in a Region of High Poultry Production, Delmarva, Maryland. Avian Diseases 61:128–134.

Ramey, A. M., A. B. Reeves, B. J. Lagassé, V. Patil, L. E. Hubbard, D. W. Kolpin, R. B. McCleskey, D. A. Repert, D. E. Stallknecht, and R. L. Poulson. 2022. Evidence for

interannual persistence of infectious influenza A viruses in Alaska wetlands. Science of The Total Environment 803:150078.

Randall, L. A., R. H. Diehl, B. C. Wilson, W. C. Barrow, and C. W. Jeske. 2011. Potential use of weather radar to study movements of wintering waterfowl: Weather Radar and Wintering Waterfowl. The Journal of Wildlife Management 75:1324–1329.

Reese, J. G., and R. Weterings. 2018. Waterfowl migration chronologies in central Chesapeake Bay during 2002–2013. The Wilson Journal of Ornithology 130:52–69.

Rijks, J. M., M. F. Leopold, S. Kühn, R. in 't Veld, F. Schenk, A. Brenninkmeijer, S. J. Lilipaly, M. Z. Ballmann, L. Kelder, J. W. de Jong, W. Courtens, R. Slaterus, E. Kleyheeg, S. Vreman, M. J. L. Kik, A. Gröne, R. A. M. Fouchier, M. Engelsma, M. C. M. de Jong, T. Kuiken, and N. Beerens. 2022. Mass Mortality Caused by Highly Pathogenic Influenza A(H5N1) Virus in Sandwich Terns, the Netherlands, 2022. Emerging Infectious Diseases 28:2538–2542.

Rohani, P., R. Breban, D. E. Stallknecht, and J. M. Drake. 2009. Environmental transmission of low pathogenicity avian influenza viruses and its implications for pathogen invasion. Proceedings of the National Academy of Sciences 106:10365–10369.

Ruiz, S., P. Jimenez-Bluhm, F. Di Pillo, C. Baumberger, P. Galdames, V. Marambio, C. Salazar, C. Mattar, J. Sanhueza, S. Schultz-Cherry, and C. Hamilton-West. 2021. Temporal dynamics and the influence of environmental variables on the prevalence of avian influenza virus in main wetlands in central Chile. Transboundary and Emerging Diseases 68:1601–1614.

Ryzhkov, A. V., and D. S. Zrnic. 2019. Radar Polarimetry for Weather Observations. Springer
Atmospheric Sciences, Springer International Publishing, Cham.
<http://link.springer.com/10.1007/978-3-030-05093-1>. Accessed 13 Apr 2022.

Sesser, K. A., M. Iglecia, M. E. Reiter, K. M. Strum, C. M. Hickey, R. Kelsey, and D. A. Skalos.
2018. Waterbird response to variable-timing of drawdown in rice fields after
winter-flooding. PLOS ONE 13:e0204800.

Sieges, M. L., J. A. Smolinsky, M. J. Baldwin, W. C. Barrow, L. A. Randall, and J. J. Buler.
2014. Assessment of bird response to the Migratory Bird Habitat Initiative using
weather-surveillance radar. Southeastern Naturalist. Volume 13.

Soda, K., Y. Tomioka, T. Usui, Y. Uno, Y. Nagai, H. Ito, T. Hiono, T. Tamura, M. Okamatsu, M.
Kajihara, N. Nao, Y. Sakoda, A. Takada, and T. Ito. 2022. Susceptibility of herons
(family: *Ardeidae*) to clade 2.3.2.1 H5N1 subtype high pathogenicity avian influenza
virus. Avian Pathology 51:146–153.

Stubbs, Q., I.-Y. Yeo, M. Lang, J. Townshend, L. Sun, K. Prestegaard, and C. Jantz. 2020.
Assessment of Wetland Change on the Delmarva Peninsula from 1984 to 2010. Journal of
Coastal Research 36:575–589.

Toennessen, R., A. Germundsson, C. M. Jonassen, I. Haugen, K. Berg, R. T. Barrett, and E.
Rimstad. 2011. Virological and serological surveillance for type A influenza in the
black-legged kittiwake (Rissa tridactyla). Virology Journal 8:21.

U.S. Geological Survey, 2023, 1 meter Digital Elevation Models (DEMs) - USGS National Map
3DEP Downloadable Data Collection: U.S. Geological Survey.

Ward, M. P., D. N. Maftei, C. L. Apostu, and A. R. Suru. 2009. Association Between Outbreaks of Highly Pathogenic Avian Influenza Subtype H5N1 and Migratory Waterfowl (Family Anatidae) Populations. Zoonoses and Public Health 56:1–9.

Wikramaratna, P. S., O. G. Pybus, and S. Gupta. 2014. Contact between bird species of different lifespans can promote the emergence of highly pathogenic avian influenza strains. Proceedings of the National Academy of Sciences 111:10767.

Xu, Y., M. Kieboom, R. J. A. van Lammeren, Y. Si, and W. F. de Boer. 2021. Indicators of site loss from a migration network: Anthropogenic factors influence waterfowl movement patterns at stopover sites. Global Ecology and Conservation 25:e01435.

Table 1 Relative importance of BRT modelled predictors of wintering waterfowl density within the Mid-Atlantic, 1 November - 15 March 2014–2023. Only predictors with mean importance ≥ 3.0 shown.

Predictor	Relative Importance By Month - Mid-Atlantic						
	November	December	January	February	March	Mean Importance	Rank
Mean Daily Temperature (Celsius)	29.72	12.24	10.36	16.28	21.23	17.97	1
Mean Daily Precipitation (mm)	12.55	7.89	7.32	17.48	14.69	11.99	2
Distance from Radar (km)	14.11	8.00	8.73	7.90	11.84	10.12	3
Wetland Proportion at 2km Scale	3.01	5.43	7.76	6.45	4.63	5.46	4
Distance from Coast (km)	2.87	5.99	5.24	4.48	5.46	4.81	5
Shrub/Scrub Proportion at 2km Scale	6.71	4.21	4.22	2.75	3.12	4.20	6
16-Day NDVI	2.36	4.37	4.47	3.61	3.54	3.67	7
Soil Wetness Index	2.34	4.25	4.47	3.59	3.18	3.57	8
Grassland Proportion at 2km Scale	2.56	4.06	4.28	2.85	3.12	3.37	9
Grain Proportion at 2km Scale	1.91	4.22	4.37	3.00	2.87	3.27	10
Open Water Proportion at 2km Scale	2.20	4.45	3.68	2.60	2.64	3.11	11
Developed Proportion at 2km Scale	2.00	3.97	4.11	3.10	2.39	3.11	12
Forest Proportion at 2km Scale	2.54	3.91	3.67	2.41	2.59	3.02	13

Table 2 Relative importance of BRT modelled predictors of wintering waterfowl density within the Central Valley of California, 1 November - 15 March 2014–2023. Only predictors with mean importance ≥ 3.0 shown. Mean importance is represented by the deviance (percent of total variation) explained by each variable and all variables combined (bottom row).

Predictor	Relative Importance By Month - California Valley of California						
	November	December	January	February	March	Mean Importance	Rank
Rice Proportion at 2km Scale	27.67	22.97	8.45	3.13	2.59	12.96	1
Ground Elevation (m)	8.00	6.57	19.53	17.62	11.23	12.59	2
Mean Daily Temperature (Celsius)	5.96	5.85	5.28	7.97	16.20	8.25	3
Distance from Radar (km)	6.01	6.16	6.20	7.17	8.01	6.71	4
Soil Wetness Index	4.06	5.67	8.08	6.29	4.82	5.78	5
Mean Daily Precipitation (mm)	3.86	4.66	5.90	4.92	6.33	5.14	6
Distance from River (km)	5.35	4.63	4.61	5.03	5.57	5.04	7
Distance to Lake (km)	4.09	3.93	4.51	5.51	6.85	4.98	8
Grassland Proportion at 2km Scale	3.47	4.10	4.67	5.71	4.65	4.52	9
Developed Proportion at 2km Scale	4.13	4.23	4.53	4.97	4.51	4.47	10
Grain Proportion 2km Scale	4.16	4.33	4.30	5.01	4.36	4.43	11
Wetland Proportion at 2km Scale	4.55	5.29	3.29	3.46	3.61	4.04	12
16-Day NDVI	3.38	3.65	4.29	4.67	4.11	4.02	13
Open Water Proportion at 2km Scale	2.65	3.10	3.10	3.38	2.96	3.04	14

Figure 1 Map showing 6 NEXRAD sites used for observing wintering waterfowl distributions 2014¬2023. Dark gray depicts the radar's 100km range. Dashed lines on the bottom left image indicate areas outside of the CVC. Light gray is outside of the radar's range.
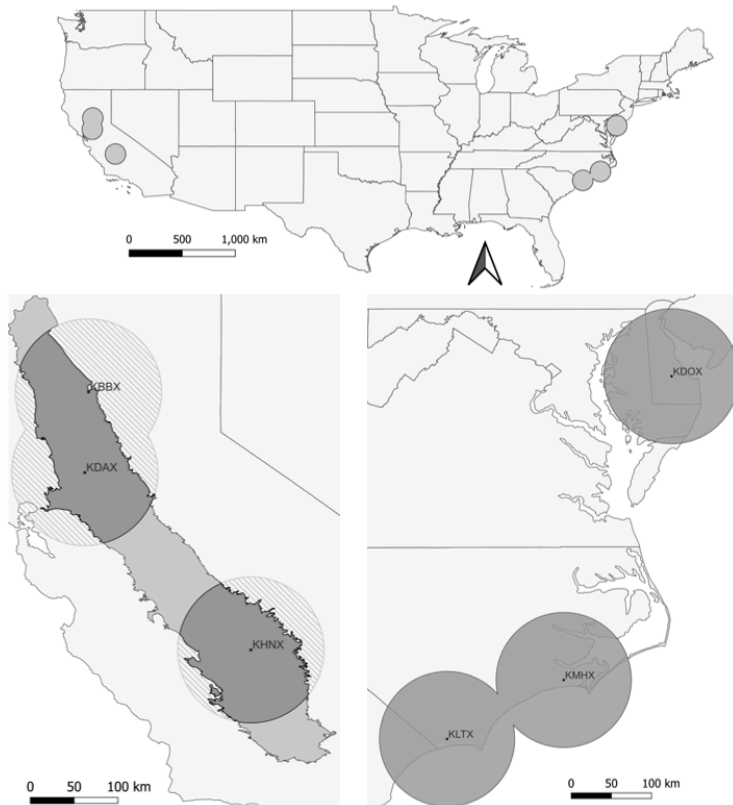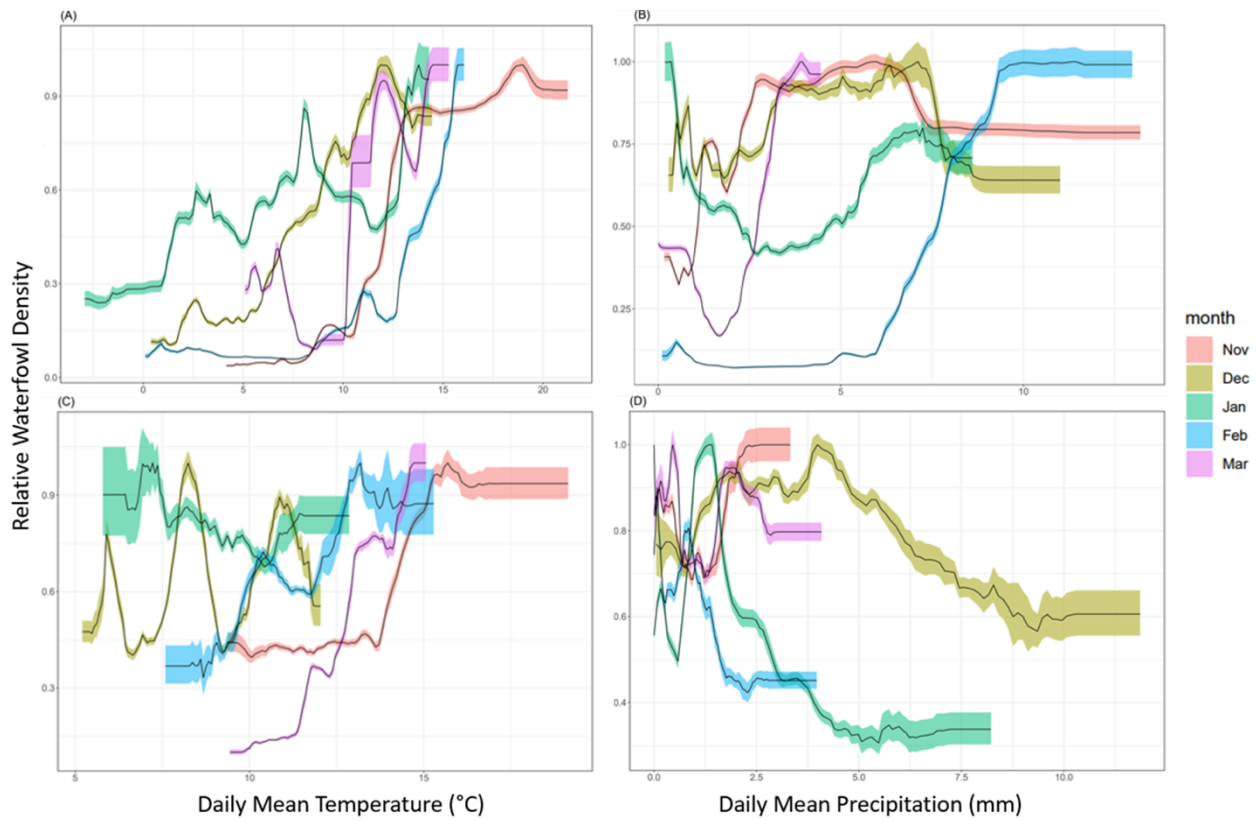
Figure 2 Mean relative waterfowl density by month (proportion of the monthly maximum of partial waterfowl density) as a function of mean daily temperature and mean daily precipitation across 25 BRT models in the MA (top: A, B) and CVC (bottom: C, D), 1 November - 15 March 2014–2023. Shading represents SE of mean response among 25 BRT models.
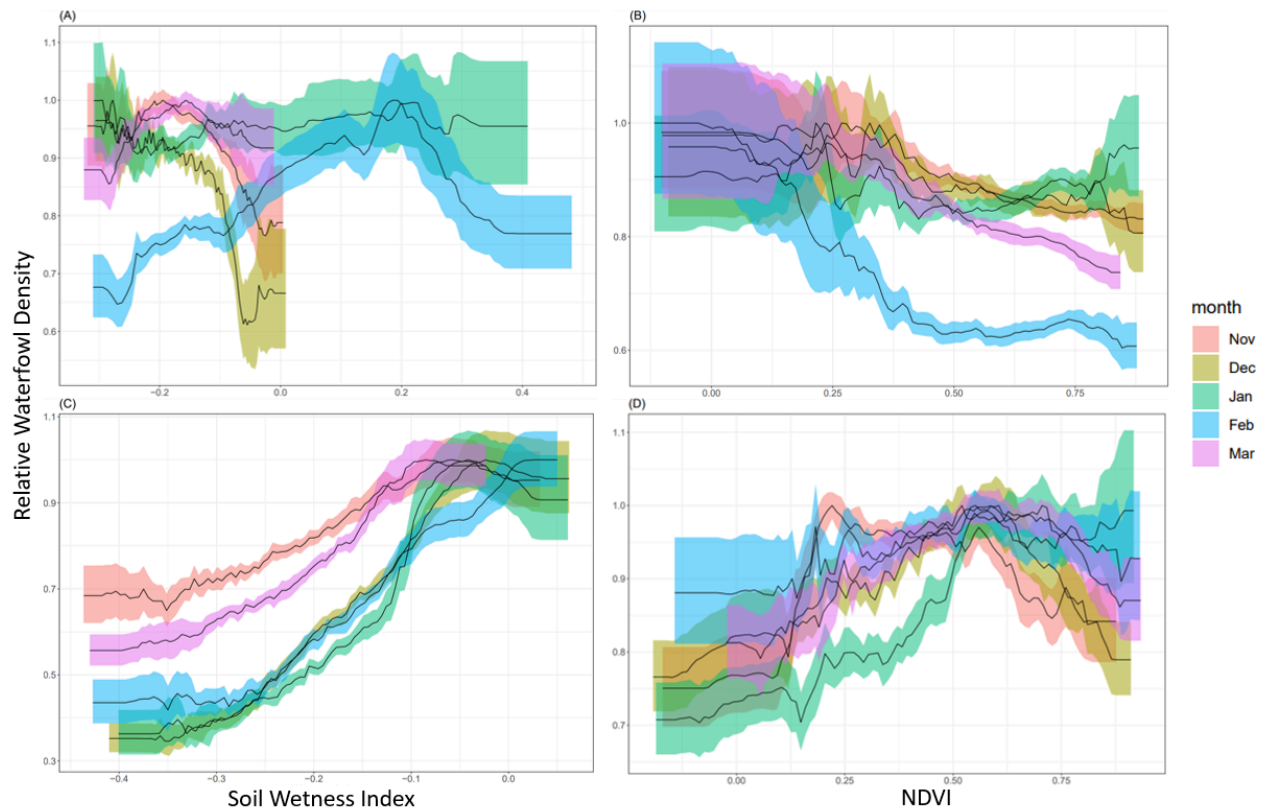
Figure 3 Mean relative waterfowl density by month (proportion of the monthly maximum of partial waterfowl density) as a function of soil wetness index and NDVI across 25 BRT models in the MA (top: A, B) and CVC (bottom: C, D), 1 November - 15 March 2014–2023. Shading represents SE of mean response among 25 BRT models.

Figure 4 Mean relative waterfowl density by month (proportion of the monthly maximum of partial waterfowl density) as a function of distance to geographic features in the MA (top: A, B, and C) and CVC (bottom: D, E, F), November - 15 March 2014–2023. Shading represents SE of mean response among 25 BRT models.
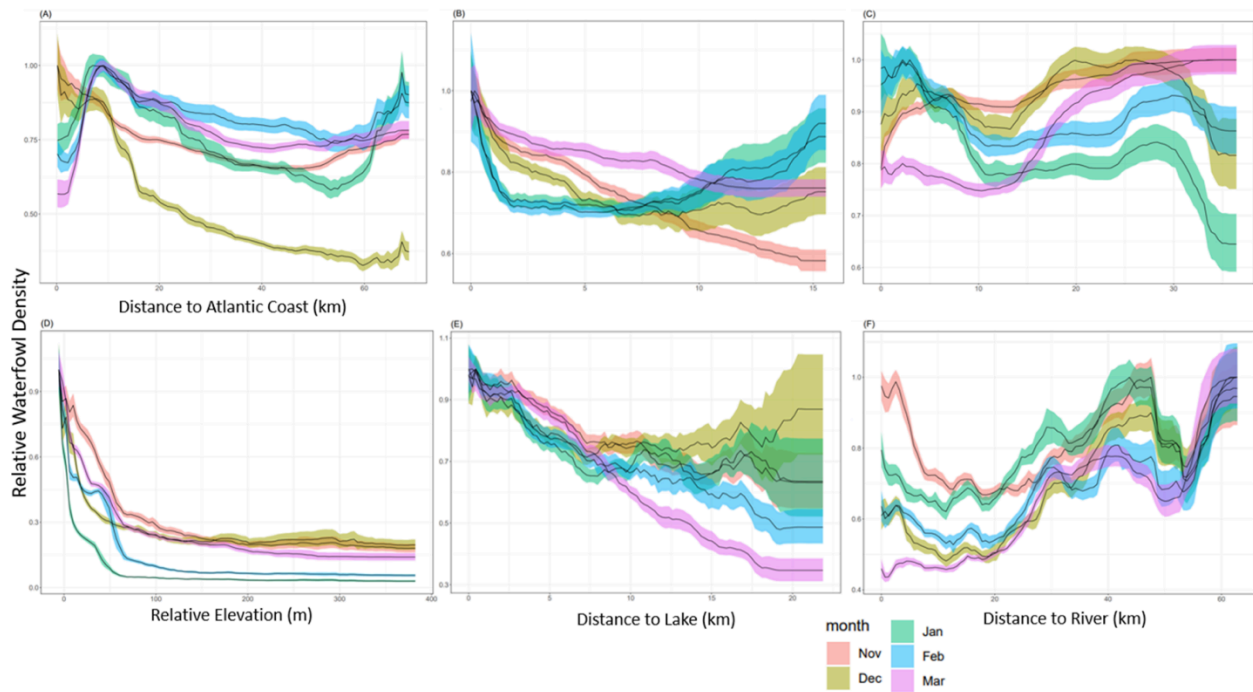
Figure 5 Mean relative waterfowl density by month (proportion of the monthly maximum of partial waterfowl density for covariance) as a function of top-9 highest ranked land cover types in the MA, 1 November - 15 March 2014–2023. Shading represents SE of mean response among 25 BRT models.
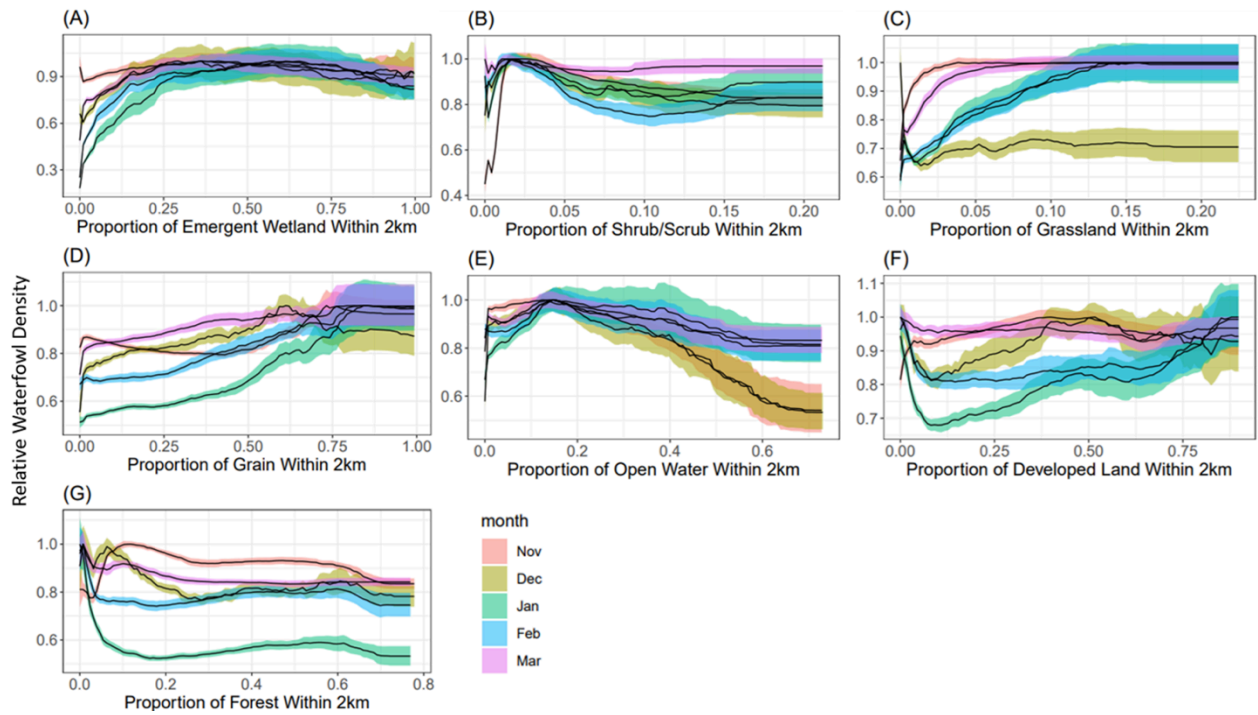
Figure 6 Mean relative waterfowl density by month (proportion of the monthly maximum of partial waterfowl density for covariance) as a function of top-9 highest ranked land cover types in the CVC, 1 November - 15 March 2014–2023. Shading represents SE of mean response among 25 BRT models.